

Learning Locality-Constrained Collaborative Representation for Face Recognition

Xi PENG^a, Lei ZHANG^{a,*}, Yi ZHANG^a, Kok Kiong Tan¹

^aMachine Intelligence Laboratory, College of Computer Science, Sichuan University, Chengdu, 610065, China.

^bDepartment of Electrical and Computer Engineering, National University of Singapore, 4 Engineering Drive 3, Singapore 117576.

Abstract

The model of low-dimensional manifold and sparse representation are two well-known concise models that suggest each data can be described by a few characteristics. Manifold learning is usually investigated for dimension reduction by preserving some expected local geometric structures from original space to low-dimensional space. The structures are generally determined by using pairwise distance, e.g., Euclidean distance. Alternatively, sparse representation denotes a data point as a linear combination of the points from the same subspace. In practical applications, however, the nearby points in terms of pairwise distance, may not belong to the same subspace, and vice versa. Consequently, it is interesting and important to explore how to get a better representation by integrating these two models together. To this end, this paper proposes a novel coding algorithm, called Locality-Constrained Collaborative Representation (LCCR), which improves the robustness and discrimination of data representation by incorporating the locality based on pairwise distance into coding process. In addition, the proposed objective function has an analytical solution, and it does not involve local minima. The empirical studies based on three public facial databases, ORL, AR and Extend Yale B, demonstrate that LCCR outperforms three state-of-the-art models, sparse representation based classification (SRC) [1], ℓ^2 -FR [2] and CRC-RLS [3] in the context of recognizing human faces from frontal views with varying expression and illumination, as well as various corruptions and occlusions.

Keywords: Non-sparse representation, Sparse representation, locality preservation, ℓ^1 -Minimization, ℓ^2 -Minimization.

1. Introduction

Sparse coding or sparse representation has become a powerful method to address problems in machine intelligence [4, 5]. It assumes that each data point $\mathbf{x} \in \mathbb{R}^m$ can be encoded as a linear combination of other points, i.e. $\mathbf{x} = \mathbf{D}\mathbf{a}$, where \mathbf{D} is a dictionary consisting of other points, and \mathbf{a} is the representation of \mathbf{x} over \mathbf{D} . If most entries of \mathbf{a} are zeros, then \mathbf{a} is called a sparse representation. Generally, it can be achieved by solving

$$(P_0) : \quad \min \|\mathbf{a}\|_0 \quad \text{s.t.} \quad \mathbf{x} = \mathbf{D}\mathbf{a},$$

where $\|\cdot\|_0$ denotes ℓ^0 -norm which counts the number of nonzero entries in a vector. P_0 is difficult to solve since it is a NP-hard problem. Recently, compressive sensing theory [6, 7, 8] have found that the solution of P_0 equals that of ℓ^1 -minimization problem, i.e.,

$$(P_{1,1}) : \quad \min \|\mathbf{a}\|_1 \quad \text{s.t.} \quad \mathbf{x} = \mathbf{D}\mathbf{a},$$

where the ℓ^1 -norm $\|\cdot\|_1$ sums the absolute value of all elements in a vector. $P_{1,1}$ is convex and can be solved by a large amount of convex optimization methods, such as basis pursuit (BP) [9], least angle regression (LARS) [10]. In [11], Yang et al. make a comprehensive survey for some popular optimizers.

*Corresponding author

Email addresses: pangsaai@gmail.co (Xi PENG), leizhang@scu.edu.cn (Lei ZHANG), zhangyi@scu.edu.cn (Yi ZHANG), kktan@nus.edu.sg (Kok Kiong Tan)

Benefiting from the emergence of compressed sensing theory, sparse coding has been widely used for various recognition tasks. Wright et al. [1] reported a remarkable method that uses sparse representation for face recognition, named SRC. They first encode a given image to a linear combination of training face images via ℓ^1 -minimization. Then they perform classification by finding which class produces the minimal reconstruction error (also called residual). SRC showed impressive accuracy and robustness, and has motivated a large amount of works in pattern recognition and machine learning, e.g., subspace learning [12, 13, 14], spectral clustering [15, 16], image classification [17], matrix factorization [18].

However, is ℓ^1 -norm based sparsity really necessary to improve the performance of face recognition? Four papers recently examined this problem. Yang et al. [19] discussed the connections and differences between ℓ^1 -optimizer and ℓ^0 -optimizer for SRC. Their theoretical analysis and experimental studies show that the success of SRC should attributes to the mechanism of ℓ^1 -optimizer which selects the set of support training samples for the given testing sample by minimizing reconstruction error. In other words, the support training samples guarantee the global similarity but sparsity which is critical for pattern recognition. Rigamonti et al. [20] compared the discrimination of two different data models. One is the ℓ^1 -norm based sparse representation, and the other model is produced by passing input into a simple convolution filter. Their result showed that two approaches achieve a similar recognition rate. Therefore, ℓ^1 -norm based sparsity is actually not as essential as it seems in the previous claims. Shi et al. [2] provided a more intuitive approach to investigate this problem by removing the ℓ^1 -regularization term from the objective function of SRC. Their experimental results showed that their method (ℓ^2 -FR) achieves a higher recognition rate than SRC if the original data is available for ℓ^2 -FR. Moreover, Zhang et al. [3] replace the ℓ^1 -norm by the ℓ^2 -norm, and their experimental results again support the views that ℓ^1 -norm based sparsity is not necessary to improve the discrimination of data representation.

As another extensively-studied concise model, manifold learning is usually investigated for dimension reduction by embedding local geometric structure of original data into a low-dimensional representation [21, 22, 23, 24, 25]. The geometric structure is generally determined by using pairwise distance, which is hardly reflected in sparse representation. As the neighboring points in terms of pairwise distance may not belong to the same subspace (sub-manifold), and vice versa, the data models based on either locality or sparsity cannot represent well the real structure of data.

To address this problem, some researchers have explored the possibility of integrating the locality with the sparsity together to produce a better data model. Richard et al. [26] successfully bridged the connections between sparse coding and manifold learning, and have founded the theory for random projections of smooth manifold; Majumdar et al. [27] investigated the effectiveness and robustness of random projection method in classification task; Peng et al. [28] proposed a method to construct a similarity graph by enforcing locality onto a non-sparse graph. These works tried to introduce sparsity into the framework of graph-oriented algorithms, have attracted a lot of attentions and achieved state-of-the-art results in subspace learning and segmentation tasks.

On the other hand, few works investigated the possibility of assimilating the geometric structure of data into the process of data modeling. To the best of our knowledge, the most similar works are: Wang et al. [29] proposed a dictionary learning method named locality-constrained linear coding (LLC) for hierarchical images classification; Chao et al. [30] presented a approach to unify group sparsity and data locality by introducing the term of ridge regression into LLC; Yang et al. [31] incorporated the prior knowledge into the coding process by iteratively learning a weight matrix of which the atoms measure the similarity between two data points.

Motivated by the assumption that similar inputs have similar codes, we propose a coding algorithm for face recognition, named Locality-Constrained Collaborative Representation (LCCR). Here, collaborative representation means that the testing sample is encoded in terms of its intra-subspace and neighboring data points. LCCR incorporates the locality based on pairwise distance into the global representation over the training data for enforcing the the representation of input could reconstruct the input and its nearby points with the minimum reconstruction error simultaneously. Note that, LCCR has an analytic solution and does not involve an alternative optimization process. The experimental results show that LCCR outperforms SRC, ℓ^1 -FR, CRC-RLS, Linear SVM on original input in accuracy and robustness in the context of face recognition.

The remainder of paper is organized as follows: Section 2 introduces three state-of-the-art works for face recognition based on data representation, i.e., SRC [1], ℓ^2 -FR [2] and CRC-RLS [3]. Section 3 presents our LCCR algorithm. Section 4 reports the experiments on facial databases. Finally, Section 5 contains the conclusion.

2. Preliminaries

2.1. Notation

We consider a set of N facial images collected from L subjects. Each training image, which is denoted as a vector $\mathbf{d}_i \in \mathbb{R}^M$, corresponds to the i th column of a dictionary $\mathbf{D} \in \mathbb{R}^{M \times N}$. Without generality, we assume that the columns of \mathbf{D} are sorted according to their labels.

Except in some specified cases, lower-case bold letters represent column vectors and upper-case bold ones represent matrices, \mathbf{A}^T denotes the transpose of the matrix \mathbf{A} , \mathbf{A}^{-1} represents the pseudo-inverse of \mathbf{A} , and \mathbf{I} is reserved for identity matrix.

2.2. Sparse representation based classification

Sparse coding aims at finding the most sparse solution of $P_{1,1}$. However, in many practical problems, the constraint $\mathbf{x} = \mathbf{D}\mathbf{a}$ cannot hold exactly since the input \mathbf{x} may include noise. Wright et al. [1] relaxed the constraint to $\|\mathbf{x} - \mathbf{D}\mathbf{a}\|_2 \leq \varepsilon$, where $\varepsilon > 0$ is the error tolerance, then, $P_{1,1}$ is rewritten as:

$$(P_{1,2}) : \quad \min \|\mathbf{a}\|_1 \quad \text{s.t.} \quad \|\mathbf{x} - \mathbf{D}\mathbf{a}\|_2 \leq \varepsilon.$$

Using Lagrangian method, $P_{1,2}$ can be transformed to the following unconstrained optimization problem:

$$(P_{1,3}) : \quad \underset{\mathbf{a}}{\operatorname{argmin}} \|\mathbf{x} - \mathbf{D}\mathbf{a}\|_2^2 + \lambda \|\mathbf{a}\|_1,$$

where the scalar $\lambda \geq 0$ balances the importance between the reconstruction error of \mathbf{x} and the sparsity of code \mathbf{a} . Given a testing sample $\mathbf{x} \in \mathbb{R}^M$, its sparse representation $\mathbf{a}^* \in \mathbb{R}^N$ can be computed by solving $P_{1,2}$ or $P_{1,3}$.

After getting the sparse representation of \mathbf{x} , one infers its label by assigning \mathbf{x} to the class that has the minimum residual:

$$r_i(\mathbf{x}) = \|\mathbf{x} - \mathbf{D} \cdot \delta_i(\mathbf{a}^*)\|_2, \quad (1)$$

$$\text{identity}(\mathbf{x}) = \underset{i}{\operatorname{argmin}} \{r_i(\mathbf{x})\}. \quad (2)$$

where the nonzero entries of $\delta_i(\mathbf{a}^*) \in \mathbb{R}^N$ are the entries in \mathbf{a}^* that are associated with i th class, and $\text{identity}(\mathbf{x})$ denotes the label for \mathbf{x} .

2.3. ℓ^2 -minimization based representation

ℓ^2 -FR [2] and CRC-RLS [3] are two recently-proposed ℓ^2 -norm based coding algorithms which achieve state-of-the-art accuracy and computational efficiency in face recognition. ℓ^2 -FR removes the ℓ^1 -regularization term from $P_{1,4}$, then the objective function becomes:

$$(\ell^2\text{-FR}) : \quad \underset{\mathbf{a}}{\operatorname{argmin}} \|\mathbf{x} - \mathbf{D}\mathbf{a}\|_2^2,$$

Moreover, a key difference between ℓ^2 -FR and SRC is that ℓ^2 -FR requires \mathbf{D} to be an over-determined matrix for achieving competitive results, while the dictionary \mathbf{D} of SRC must be under-determined to satisfy the conditions of compressive sensing. Once the optimal code \mathbf{a}^* is calculated for a given input, the classifier (1) and (2) is used to determine the label for the input \mathbf{x} .

CRC-RLS estimates the representation \mathbf{a}^* for the input \mathbf{x} by relaxing the ℓ^1 -norm to the ℓ^2 -norm in $P_{1,3}$. They aimed to solve following objective function:

$$(\text{CRC-RLS}) : \quad \underset{\mathbf{a}}{\operatorname{argmin}} \|\mathbf{x} - \mathbf{D}\mathbf{a}\|_2^2 + \lambda \|\mathbf{a}\|_2^2,$$

where $\lambda > 0$ is a balance factor.

ℓ^2 -FR and CRC-RLS show that ℓ^2 -norm based data models can achieve competitive classification accuracy with hundreds of times speed increase, compared with SRC. Under this background, we aim to incorporate the local geometric structures into coding process for achieving better discrimination and robustness.

3. Locality-Constrained Collaborative Representation

It is a big challenge to improve the discrimination and the robustness of facial representation because a practical face recognition system requires not only a high recognition rate but also the robustness against various noise and occlusions. As two of the most promising methods, locality preservation based algorithm and sparse representation have been extensively studied and successfully applied to appearance-based face recognition, respectively. Locality preservation based algorithm aims to find a low-dimensional model by preserving local neighborhood from original space to another one. It is derived from the assumption of manifold learning that the neighborhood of each point is homeomorphic to the Euclidean space if the data is well sampled from a smooth manifold. Alternatively, sparse representation, which encodes each testing sample as a linear combination of the training data, depicts a global relationship between testing sample with training ones. In this paper, we aim to integrate the locality based on pairwise distance with the global property derived from coding scheme together for modeling facial data. Our objective function is in the form of

$$E(\mathbf{x}, \mathbf{a}) = \|\mathbf{x} - \mathbf{D}\mathbf{a}\|_2^2 + \lambda \|\mathbf{a}\|_p + \gamma E_L, \quad (3)$$

where $p = \{1, 2\}$, E_L is the locality constraint, $\lambda \geq 0$ and $\gamma \geq 0$ dictate the importance of $\|\cdot\|_p$ and E_L , respectively. Then the key is to formulate the geometric property of the neighborhood into E_L .

Naturally, E_L can be defined as the reconstruction error of the neighborhood of the testing image, i.e.,

$$E_L(\mathbf{Y}(\mathbf{x}), \mathbf{C}) = \frac{1}{K} \sum_{\substack{\mathbf{y}_i(\mathbf{x}) \in \mathbf{Y}(\mathbf{x}) \\ \mathbf{c}_i \in \mathbf{C}}} \|\mathbf{y}_i(\mathbf{x}) - \mathbf{D}\mathbf{c}_i\|_2^2, \quad (4)$$

where, for an input $\mathbf{x} \in \mathbb{R}^M$, its neighborhood $\mathbf{Y}(\mathbf{x}) \in \mathbb{R}^{M \times K}$ is searched from the training samples according to prior knowledge or manual labeling. For simplicity, we assume that each data point has K neighbors, and $\mathbf{c}_i \in \mathbb{R}^N$ denotes the optimal code for $\mathbf{y}_i(\mathbf{x})$.

To bridge the connection between the objective variant \mathbf{a} and \mathbf{c}_i , one assumes that \mathbf{a} could be represented as a linear combination of the $\{\mathbf{c}_i\}_{i=1}^K$. Mathematically,

$$\mathbf{a} = \sum_{\mathbf{c}_i \in \mathbf{C}} \mathbf{w}_i^T \mathbf{c}_i,$$

where $\mathbf{w}_i \in \mathbb{R}^N$ is the similarity between \mathbf{a} and \mathbf{c}_i . The calculation of \mathbf{w}_i is a challenging and key step which has been studied in many works [29, 31]. Most of these works get an optimal \mathbf{w}_i via an iterative calculation process which increases additional computational costs. Moreover, another difference between our work and these works is that we aim to denote \mathbf{a} with \mathbf{c}_i , not vice versa.

Here, we present a simple but effective method to solve this problem by directly replacing \mathbf{c}_i with \mathbf{a} . This is based on an assumption that the representation of \mathbf{x} also can approximate the representation of \mathbf{y}_i , i.e.,

$$\|\mathbf{y}_i - \mathbf{D}\mathbf{c}_i\|_2^2 \leq \|\mathbf{y}_i - \mathbf{D}\mathbf{a}\|_2^2 \leq \|\mathbf{y}_i - \mathbf{D}\bar{\mathbf{a}}\|_2^2,$$

where $\bar{\mathbf{a}}$ denotes the representation of the point which is not close to \mathbf{y}_i .

Figure 1 show an example to illustrate the validity of our motivation. There are three face images A , B and C selected from two different individuals, where A and B came from the same person. This means that A and B lie on the same subspace and can represent each other with less reconstruction error. Figure 1(b) is a practical example corresponding to Figure 1(a). Either from the Eigenface matrices or the coefficients of the two coding schemes, we can see that the similarity between A and B is much higher than the similarity between C and either of them.

Based on the above discussions, we propose an objective function as follows:

$$\begin{aligned} E(\mathbf{x}, \mathbf{Y}(\mathbf{x}), \mathbf{a}) = & (1 - \gamma) \|\mathbf{x} - \mathbf{D}\mathbf{a}\|_2^2 \\ & + \gamma \frac{1}{K} \sum_{\mathbf{y}_i(\mathbf{x}) \in \mathbf{Y}(\mathbf{x})} \|\mathbf{y}_i - \mathbf{D}\mathbf{a}\|_2^2 + \lambda \|\mathbf{a}\|_p, \end{aligned} \quad (5)$$

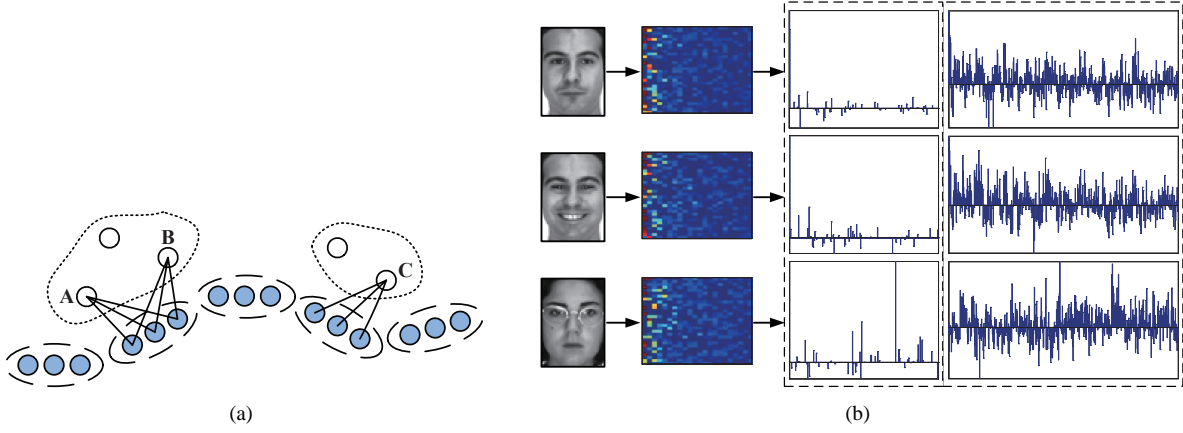


Figure 1: The key observation is that the representations of nearby points are more similar than that of non-neighboring points. (a) Three face images from two different sub-manifolds are linked to their corresponding neighbors respectively. (b) The first column includes three images which correspond to the points A , B and C in Figure 1(a); The second column shows the Eigenface feature matrices for the test images; The third column includes two parts: the left part is them code coefficients for SRC, and the right one is for CRC-RLS.

where $0 \leq \gamma \leq 1$ balances the importance between the testing image \mathbf{x} and its neighborhood $\mathbf{Y}(\mathbf{x})$. The second term, which measures the contribution of locality, can largely improve the robustness of \mathbf{a} . If \mathbf{x} is corrupted by noise or occluded by disguise, a larger γ will yield better recognition results. In addition, we can find that SRC, CRC-RLS and ℓ^2 -FR are three simple and special forms of our algorithm when $\gamma = 0$, $p = 1$, and $\gamma = 0$, $p = 2$, as well as $\lambda = 0$, $\gamma = 0$, $p = 2$, respectively.

Consider the recent findings, i.e., ℓ^1 -norm based sparsity cannot bring higher recognition accuracy and better robustness for facial data than ℓ^2 -norm based methods [2, 3], we simplify our objective function (5) as follows:

$$\begin{aligned} E(\mathbf{x}, \mathbf{Y}(\mathbf{x}), \mathbf{a}) = & (1 - \gamma) \|\mathbf{x} - \mathbf{D}\mathbf{a}\|_2^2 \\ & + \gamma \frac{1}{K} \sum_{\mathbf{y}_i(\mathbf{x}) \in \mathbf{Y}(\mathbf{x})} \|\mathbf{y}_i(\mathbf{x}) - \mathbf{D}\mathbf{a}\|_2^2 + \lambda \|\mathbf{a}\|_2^2, \end{aligned} \quad (6)$$

Clearly, (6) achieves the minimum when its derivative with respect to \mathbf{a} is zero. Hence, the optimal solution is

$$\mathbf{a}^* = (\mathbf{D}^T \mathbf{D} + \lambda \cdot \mathbf{I})^{-1} \mathbf{D}^T \left[(1 - \gamma) \mathbf{x} + \gamma \frac{1}{K} \sum_{\mathbf{y}_i(\mathbf{x}) \in \mathbf{Y}(\mathbf{x})} \mathbf{y}_i(\mathbf{x}) \right]. \quad (7)$$

Let $\mathbf{P} = (\mathbf{D}^T \mathbf{D} + \lambda \cdot \mathbf{I})^{-1} \mathbf{D}^T$ whose calculation requires re-formulating the psuedo-inverse. Clearly, \mathbf{P} can be calculated in advance and only once as it is only dependent on training data \mathbf{D} ,

Given a testing image \mathbf{x} , the first step is to determine its neighborhood $\mathbf{Y}(\mathbf{x})$ from the training set according to prior knowledge, or manual labeling, etc. In practical applications, there are two widely-used variations for finding the neighborhood:

1. ϵ -neighborhoods. The training sample \mathbf{d}_i is a neighbor of the testing image \mathbf{x} if $\|\mathbf{d}_i - \mathbf{x}\|_2 < \epsilon$, where $\epsilon > 0$ is a constant.
2. K -nearest neighbors (K -NN). The training sample \mathbf{d}_i is a neighbor of \mathbf{x} , if \mathbf{d}_i is among the K -nearest neighbors of \mathbf{x} , where $K > 0$ can be specified as a constant or determined adaptively.

The two variations involve a choice of distance metrics. A lot of baselines are available, for example, Euclidean distance. In addition, supervised distance metric learning [32], which makes use of label information to identify correlations between dimensions, has shown significantly improvement of the accuracy of K -NN searching.

Once the neighborhood of the testing image \mathbf{x} is obtained, LCCR just simply projects \mathbf{x} and its neighborhood $\mathbf{Y}(\mathbf{x})$ onto space \mathbf{P} via (7). Thus, LCCR is quite fast. In addition, the matrix form of LCCR is easily derived, which can

used in batch processing.

$$\mathbf{A}^* = (\mathbf{D}^T \mathbf{D} + \lambda \cdot \mathbf{I})^{-1} \mathbf{D}^T \left[(1 - \gamma) \mathbf{X} + \gamma \frac{1}{K} \sum_{i=1}^K \mathbf{Y}_i(\mathbf{X}) \right],$$

where the columns of $\mathbf{X} \in \mathbb{R}^{M \times J}$ are the testing images whose codes are stored in $\mathbf{A}^* \in \mathbb{R}^{N \times J}$, and $\mathbf{Y}_i(\mathbf{X}) \in \mathbb{R}^{M \times J}$ denotes the collection of i th-nearest neighbor of \mathbf{X} .

The proposed LCCR algorithm is summarized in Algorithm 1, and an overview is illustrated in Figure 2.

Algorithm 1 Face Recognition using Locality-Constrained Collaborative Representation (LCCR)

Input: A matrix of training samples $\mathbf{D} = [\mathbf{d}_1, \mathbf{d}_2, \dots, \mathbf{d}_N] \in \mathbb{R}^{M \times N}$ which are sorted according to the label of \mathbf{d}_i , $1 \leq i \leq N$; A testing image $\mathbf{x} \in \mathbb{R}^M$; The balancing factors $\lambda \geq 0$ and $0 \leq \gamma \leq 1$.

- 1: Normalize the columns of \mathbf{D} and \mathbf{x} to have a unit ℓ^2 -norm, respectively.
- 2: Calculate the projection matrix $\mathbf{P} = (\mathbf{D}^T \mathbf{D} + \lambda \cdot \mathbf{I})^{-1} \mathbf{D}^T$ and store it.
- 3: Find the neighborhood $\mathbf{Y}(\mathbf{x}) = \{\mathbf{y}_1(\mathbf{x}), \mathbf{y}_2(\mathbf{x}), \dots, \mathbf{y}_K(\mathbf{x})\}$ for \mathbf{x} from training samples \mathbf{D} .
- 4: Code \mathbf{x} over \mathbf{D} via

$$\mathbf{a}^* = \mathbf{P} \cdot \left[(1 - \gamma) \mathbf{x} + \gamma \frac{1}{K} \sum_{\mathbf{y}_i(\mathbf{x}) \in \mathbf{Y}(\mathbf{x})} \mathbf{y}_i(\mathbf{x}) \right].$$

- 5: Compute the regularized residuals over all classes by

$$r_i(\mathbf{x}) = \frac{\|\mathbf{x} - \mathbf{D} \cdot \delta_i(\mathbf{a}^*)\|_2}{\|\delta_i(\mathbf{a}^*)\|_2},$$

where i denotes the index of class.

Output: $\text{identity}(\mathbf{x}) = \text{argmin}_i \{r_i(\mathbf{x})\}$.

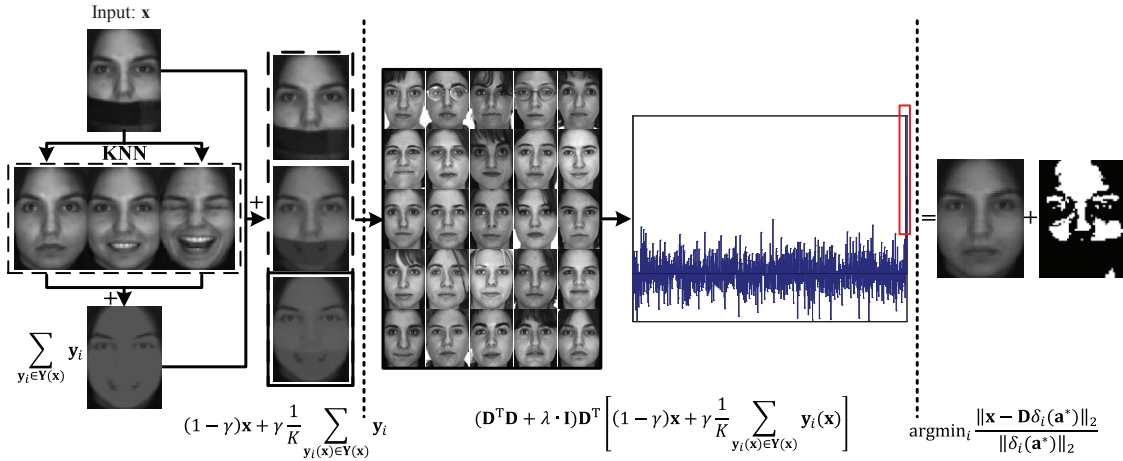


Figure 2: Overview of the coding process of LCCR, which consists of three steps separated by dotted lines. First, for a given input \mathbf{x} , find its neighborhood $\mathbf{Y}(\mathbf{x})$ from training data. Then, code \mathbf{x} over \mathbf{D} by finding the optimal representation \mathbf{a} (see bar graph) which produces the minimal reconstruction errors for \mathbf{x} and $\mathbf{Y}(\mathbf{x})$ simultaneously. Finally, conduct classification by finding which class produces the minimum residual. In the middle part of the figure, we use a red rectangles to indicate the basis vectors which produce the minimum residual.

4. Experimental Verification and Analysis

In this section, we report the performance of LCCR over three publicly-accessed facial databases, i.e., AR [33], ORL [34] and the Extended Yale database B [35], of which the images are captured in constrained environments.

There are some challenging unconstrained face data for classification, e.g., FERET [36], FRGC [37]. However, as the recent works on facial data representation [1, 2, 3], we examine the performance comparison between LCCR and these three coding schemes with respect to 1) discrimination, 2) robustness to corruptions, 3) and robustness to occlusions.

4.1. Experimental Configuration

We compare the classification results of LCCR with three state-of-the-art coding algorithms, i.e., SRC [1], ℓ^2 -FR [2] and CRC-RLS [3], as well as the result of linear SVM [38] on the original input. Note that, LCCR, SRC, ℓ^2 -FR and CRC-RLS directly code each testing sample over training data without usability of dictionary learning method, and get classification result by finding which subject produces minimum reconstruction error. In these four models, only LCCR incorporates locality based pairwise distance into coding scheme. For a comprehensive comparison, we report the performance of LCCR with five basic distance metrics, i.e., Euclidean distance (ℓ^2 -distance), Seuclidean distance (standardized Euclidean distance), Cosine distance (the cosine of the angle between two points), Cityblock distance (ℓ^1 -distance), and Spearman distance.

We get the sparse code of SRC by using the CVX [39], a package for solving convex optimization problems, and the non-sparse representations of ℓ^2 -FR and CRC-RLS by using the source code from the homepages of corresponding authors. All experiments are carried out using Matlab 32bit on a 2.5GHz machine with 2.00 GB RAM.

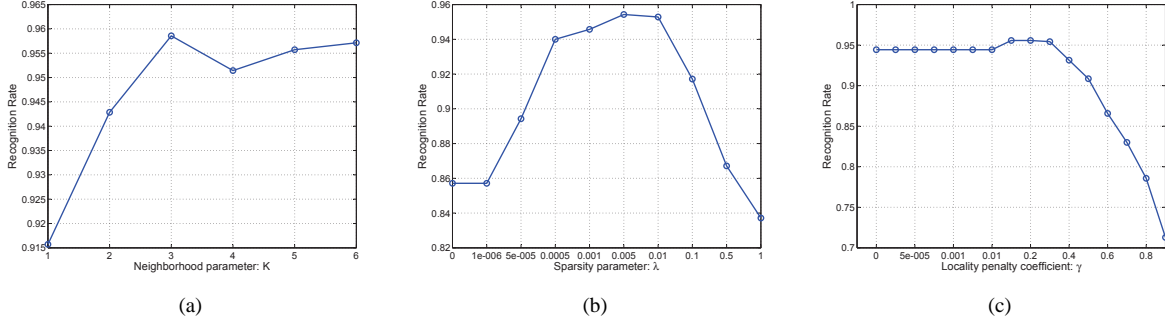


Figure 3: Recognition accuracy of LCCR using Cityblock distance on a subset of AR database with dimensionality 2580. (a) The recognition rates versus the variation of the neighborhood parameter K , where $\lambda = 0.005$ and $\gamma = 0.2$. (b) The recognition rates versus the variation of the sparsity parameter λ , where $K = 5$ and $\gamma = 0.2$. (c) The recognition rates versus the variation of the locality constrained coefficient γ , where $K = 3$ and $\lambda = 0.005$.

Parameter determination is a big challenge in pattern recognition and computer vision. As in [15, 28], we report the best classification results of all tested methods under different parameter configurations. The values tested for the parameters to find the best values for LCCR can be inferred from Figure 3, and these possible values of λ also are tested for SRC and CRC-RLS. In all tests, we randomly split each database into two parts for training and testing, and compare the performance of the algorithms using the same partition to avoid the difference of data sets.

4.2. Recognition on Clean Images

In this sub-section, we examine the performance of five competing methods using three clean facial data sets. Here, clean image means an image without occlusion or corruption, just with variations in illumination, pose, expression, etc.

4.2.1. ORL database

The ORL database consists of 400 different images of 40 individuals. For each person, there are 10 images with the variation of lighting, facial expression and facial details (with or without glasses). For computational efficiency, we cropped all ORL images from 112×96 to 56×48 , and randomly selected 5 images from each subject for training and used the remaining 5 images for testing. Table 1 reports the classification accuracy of the tested algorithms over various dimensionality. Note that, the Eigenface with 200D retains 100% energy of cropped data, which makes the investigated methods achieve the same rates over the data space with 2688D. From the results, LCCRs outperform the other algorithms, and the best results are achieved when Cityblock distance is used to search the nearest neighbors.

Moreover, there is an interesting result that except ℓ^2 -FR, the other algorithms achieve a higher recognition rate with the increase of dimensionality. The possible reason is that the cropped operation play a negative role to ℓ^2 -FR, while Eigenface increases the discrimination of model. In the following experiments, we will observe the same phenomenon.

Table 1: The Maximal Recognition Accuracy of Competing Algorithms on the ORL Database.

Dim	54	120	200	2688
SVM [38]	90.00%	92.50%	93.50%	93.00%
SRC [1]	92.00%	96.50%	86.00%	-
ℓ^2 -FR [2]	92.50%	91.00%	89.00%	89.00%
CRC-RLS [3]	94.50%	94.00%	94.50%	95.00%
LCCR + Cityblock	97.50%	97.50%	98.00%	98.00%
LCCR + Seucclidean	96.00%	96.50%	96.00%	96.50%
LCCR + Euclidean	96.00%	96.00%	96.50%	96.50%
LCCR + Cosine	96.00%	96.50%	96.50%	96.50%
LCCR + Spearman	96.00%	96.00%	96.00%	96.00%

4.2.2. AR database

The AR database includes over 4000 face images of 126 people (70 male and 56 female) which vary in expression, illumination and disguise (wearing sunglasses or scarves). Each subject has 26 images consisting of 14 clean images, 6 images with sunglasses and 6 images with scarves. As in [1, 3], a subset that contains 1400 normal faces randomly selected from 50 male subjects and 50 female subjects, is used in our experiment. For each subject, we randomly permute the 14 images and take the first half for training and the rest for testing. Limited by the computational capabilities, as in [3], we crop all images from original 165×120 to 60×43 (2580D) and convert it to gray scale.

SRC [1] and CRC-RLS [3] achieved the classification result by extracting eigenface (PCA) with 54D, 120D and 300D from cropped data, which means the dictionary \mathbf{D} is an under-determined matrix. ℓ^2 -FR [2] reported the results for the original data, which means \mathbf{D} is an over-determined matrix. For a extensive comparison, we investigate the performance of the tested methods over two cases except SRC on the latter one, since SRC requires \mathbf{D} to be an under-determined matrix.

From Table 2, we can see that LCCRs are superior to SVM, SRC, ℓ^2 -FR and CRC-RLS with respect to all examined dimensionality, and SRC achieves the second best result.

Table 2: The Maximal Recognition Accuracy of Competing Algorithms on the AR Database.

Dim	54	120	300	2580
SVM [38]	73.43%	81.00%	82.00%	83.14%
SRC [1]	81.71%	88.71%	90.29%	-
ℓ^2 -FR [2]	80.57%	90.14%	93.57%	82.29%
CRC-RLS [3]	80.57%	90.43%	94.00%	94.43%
LCCR + Cityblock	86.14%	92.71%	95.14%	95.86%
LCCR + Seucclidean	85.00%	91.86%	94.43%	95.43%
LCCR + Euclidean	84.00%	91.29%	94.14%	94.86%
LCCR + Cosine	83.43%	90.86%	94.00%	94.57%
LCCR + Spearman	84.71%	90.71%	94.14%	94.43%

4.2.3. Extended Yale B database

The database contains 2414 frontal-face images with size 192×168 over 38 subjects, as in [1, 3], we conduct experiments on the cropped and normalized images of size 54×48 . For each subject (about 64 images per subject), we randomly split the images into two parts with equal size, one for training, and the other for testing. Similar to the above experimental configuration, we calculate the recognition rates over the Eigenface spaces with dimensionality 54, 120 and 300, and full dimensional space with 2592D. From Table 3, it is clear that LCCRs again outperform its counterparts across various spaces, especially when the Spearman distance is used to determine the neighborhood of testing samples.

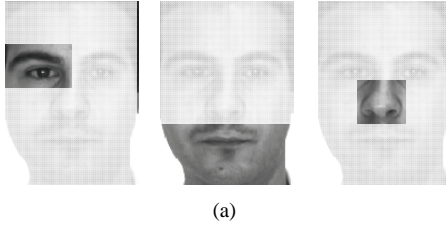
Based on the results on ORL, AR, and Extended Yale B, we draw following conclusions:

Table 3: The Maximal Recognition Accuracy of Competing Algorithms on the Extended Yale B Database.

Dim	54	120	300	2592
SVM [38]	84.52%	92.72%	95.28%	95.45%
SRC [1]	93.71%	95.12%	96.44%	-
ℓ^2 -FR [2]	92.88%	95.61%	97.85%	90.48%
CRC-RLS [3]	92.96%	95.69%	97.90%	98.26%
LCCR + Cityblock	93.21%	96.03%	97.93%	98.34%
LCCR + Seclidean	93.21%	95.70%	97.93%	98.34%
LCCR + Euclidean	93.21%	95.70%	97.93%	98.34%
LCCR + Cosine	93.46%	95.78%	97.93%	98.59%
LCCR + Spearman	97.02%	98.18%	99.10%	99.59%

1. For all databases used, LCCRs outperforms SVM (original input), SRC (sparse code), ℓ^2 -FR (non-sparse representation) and CRC-RLS (collaborative representation) over the all tested dimensionalities.
2. LCCR perform better for low-dimensional data than high-dimensional ones. For example, on the Extended Yale B, the maximal rate difference between LCCR and CRC-RLS (the second best method) changed from 4.06% with 54D, to 2.49% with 120D, and to 1.17% with 300D. It again corroborates our claim that locality based on pairwise is helpful to improving the discrimination of data representation, since the low-dimensional data contain few information than higher one.
3. SRC outperform ℓ^2 -FR and CRC-RLS over the low-dimensional feature spaces, which is consistent with the reports in [3]. CRC-RLS and ℓ^2 -FR achieve similar recognition rates with the difference less than 1% across various feature spaces.

4.3. Recognition on Partial Facial Features



(a)

Features	Right Eye	Mouth and Chin	Nose
Dim	308	798	224
SVM [38]	70.71%	41.29%	37.14%
SRC [1]	84.00%	70.71%	78.00%
ℓ^2 -FR [2]	72.86%	32.86%	70.57%
CRC-RLS [3]	83.14%	73.86%	73.57%
LCCR + Cityblock	86.86%	76.29%	75.86%
LCCR + Seclidean	84.86%	75.57%	75.29%
LCCR + Euclidean	85.29%	75.00%	76.00%
LCCR + Cosine	84.43%	74.57%	75.29%
LCCR + Spearman	84.57%	75.86%	75.14%

(b)

Figure 4: Recognition Accuracy with partial face features. (a) An example of the three features, right eye, mouth and chin, and nose from left to right. (b) The recognition rates of competing methods on the partial face features of the AR database.

The ability to work on partial face features is very interesting since not all facial features play an equal role in recognition. Therefore, this ability has become an important metric for the recognition algorithm [40]. We examine the performance of the tested methods on three partial facial features, i.e., right eye, nose, as well as mouth and chin, sheared from the clean AR faces with 2580D (as shown in Figure 4(a)). For each partial face feature, we generate a data set by randomly selecting 7 images per subject for training and the remaining 700 for testing. It should be noted that [1] conducted similar experiment on Extended Yale B which includes less subjects, smaller irrelevant white background, and more training samples per subject than our case.

Figure 4(b) shows that the proposed LCCRs achieve better recognition rates than SVM, SRC, ℓ^2 -FR and CRC-RLS for right eye as well as mouth and chin, and the second best rates for the nose. Some works found that the most important feature is the eye, followed by the mouth, and then the nose [41]. We can see that the results for SVM, CRC-RLS and LCCR are consistent with these studies although the dominance of the mouth and chin over the nose is not very distinct.

4.4. Face Recognition with Block Occlusions

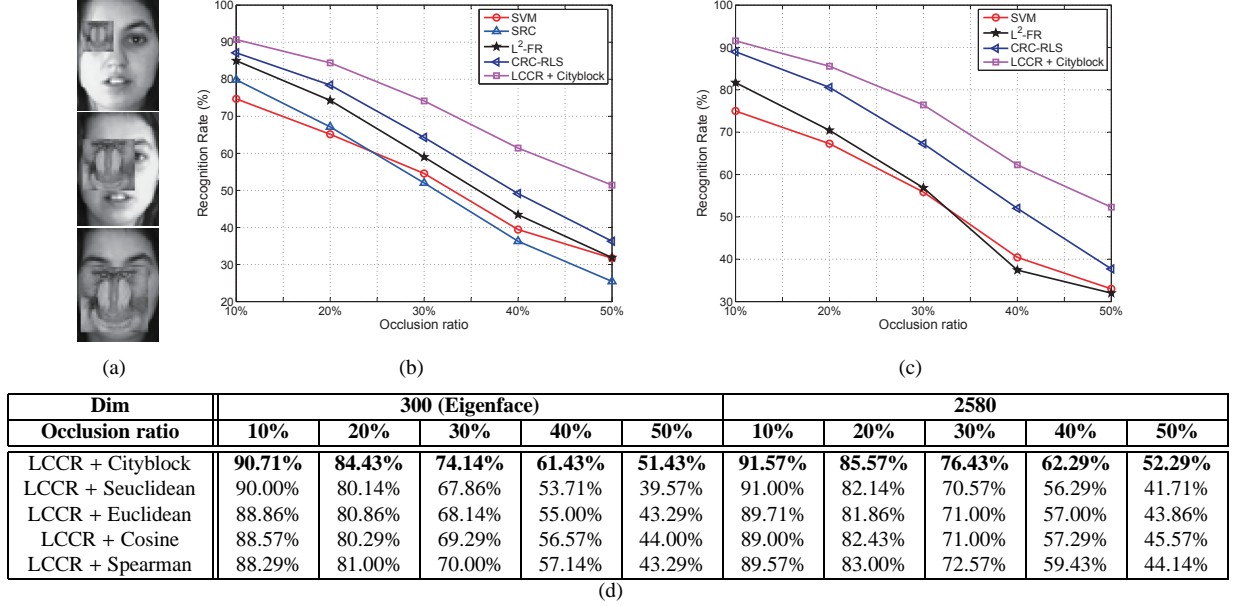


Figure 5: Experiments on AR database with varying percent block occlusion. (a) From top to bottom, the occlusion percents for test images are, 10%, 30%, and 50%, respectively. (b) and (c) are the recognition rates under different levels of block occlusion on AR database with 300D (Eigenface) and 2580D, respectively. (d) The recognition rates of LCCRs which outperform the other tested models.

To examine the robustness to block occlusion, similar to [1, 2, 3], we get 700 testing images by replacing a random block of each clean AR image with an irrelevant image (baboon) and use 700 clean images for training. The occlusion ratio increases from 10 percent to 50 percent, as shown in Figure 5(a). We investigate the classification accuracy of all tested methods over Eigenface space with 300D (Figure 5(b)) and cropped data space with 2580D (Figure 5(c)).

Figure 5(b) and Figure 5(c) show that LCCRs again outperform the other models with considerable performance margins. Especially, with the increase of the occlusion ratio, the difference of recognition rates between LCCRs and the other methods becomes larger. For example, when the occlusion ratio is 50%, in 300 dimensional space, the accuracy of LCCR with Cityblock distance is about 20% higher than SVM, about 26% higher than SRC, about 20% higher than ℓ^2 -FR, and about 15% higher than CRC-RLS.

On the other hand, it is easy to find that ℓ^2 -FR, CRC-RLS and LCCRs are more robust than SRC and SVM, which implies that the ℓ^1 -regularization term cannot yield better robustness than the ℓ^2 -regularization term, at least for the Eigenface space. Moreover, all models achieve better results in higher dimensional space, although the difference of classification accuracy between higher dimensional space and lower ones is less than 1%.

4.5. Face Recognition with Real Occlusions

In this sub-section, we examine the robustness to real possible occlusions of competing methods by using the AR database distributed over 100 individuals. We use 1400 clean images for training, 600 faces wearing by sunglasses (occluded ratio is about 20%) and 600 face wearing by scarves (occluded ratio is about 40%) for testing, separately. In [1], Wright et al. only used a third of disguised images for this test, i.e., about 200 images for each kind of disguise. In addition, this sub-section investigate the relationship between the effectiveness of K -NN searching and that of LCCR.

We examine two widely-used feature schemes [1, 3, 31], namely, the holistic feature with 54D, 300D and 2580D, as well as the partitioned feature based on the cropped data with 2580D. The partitioned feature scheme firstly partitions an image into multiple blocks (8 blocks in our case as did in [1, 3, 31], see Figure 6(a) and 6(c)), then conducts classification on each block independently, and after that, aggregates the results by voting.

Figure 6(e) reports the recognition rates of all tested methods. For the images occluded by sunglasses, LCCR with Cityblock distance achieves remarkable results with the holistic feature scheme, its recognition accuracy are nearly

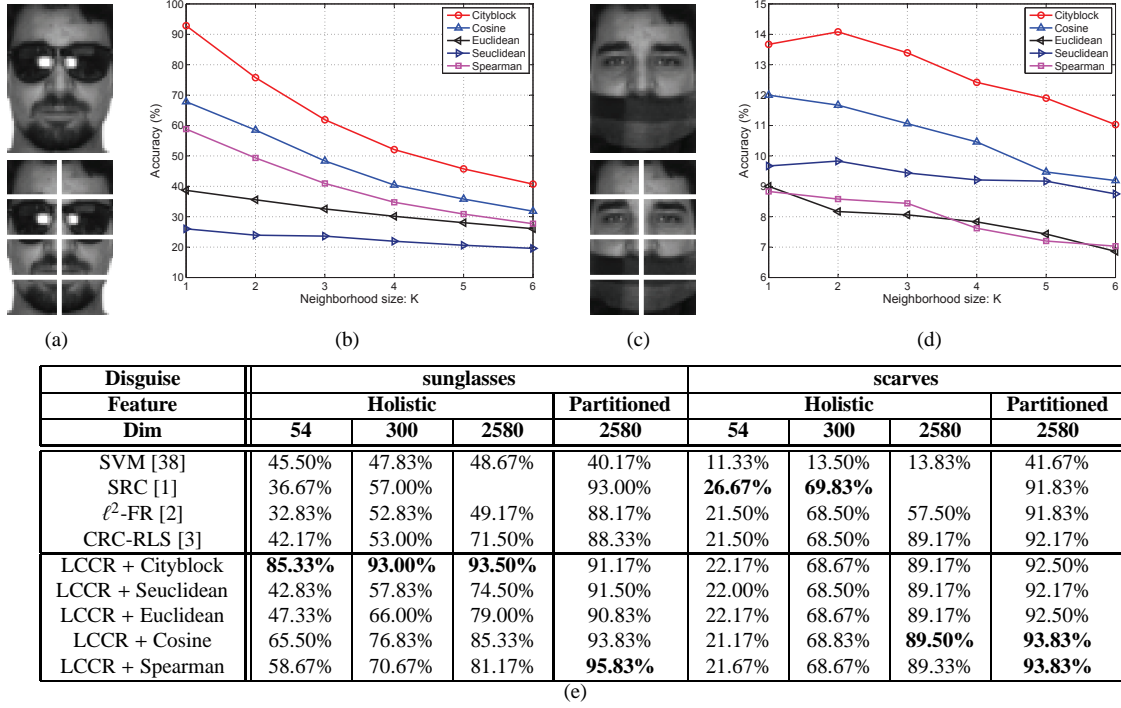


Figure 6: Recognition on AR faces with real possible occlusions. (a) The top row is a facial image occluded by sunglasses, whose partitioned blocks are shown as below. (b) The accuracy of K -NN searching using Cityblock distance, Cosine distance, Euclidean distance, Seucclidean distance and Spearman distance on the AR images with sunglasses (2580D). (c) Similar to (a), the top row is a face occluded by scarf, and its partitions below. (d) The precision of K -NN searching using Cityblock, Cosine, Euclidean, Seucclidean, Spearman as distance metrics on the AR images with scarves (2580D). (e) The recognition rates of competing methods across different experimental configurations.

double that of the other methods. This considerable performance margin contributes to that the locality based on Cityblock distance and largely improves the discrimination of representation when traditional coding scheme cannot work well (see Figure 6(b)). For the images occluded by scarves, LCCR achieves the highest recognition rate over the full dimensional space, and the second highest rates using Eigenface. However, the difference in rates between LCCR and other non-iterative algorithms (ℓ^2 -FR, CRC-RLS) is very small due to the poor accuracy of K -NN searching as shown in Figure 6(d). Furthermore, the partitioned feature provides higher recognition rates than the holistic one for all competing methods, which is consistent with previous report [1].

From the above experiments, it is easy to conclude that the preservation of locality is helpful to coding scheme, especially when the real structures of data cannot be found by traditional coding scheme. Moreover, the performance ranking of LCCR with five distance metrics is same with that of K -NN searching in terms of these metrics.

4.6. Face Recognition with Corruption

We test the robustness of LCCR against two kinds of corruption using the AR data set containing 2600 images of 100 individuals. For each subject, we use 13 images for training (7 clean images, 3 images with sunglasses, and 3 images with scarves), and the remaining 13 images for testing. Different from [1] which tested the robustness to corruption using the Extended Yale B database, our case is more challenging for the following reasons. Firstly, AR images contain real possible occlusions, i.e., sunglasses and scarves, while Extended Yale B is a set of clean images without disguises. Secondly, AR includes more facial variations (13 versus 9), more subjects (100 versus 38), and a smaller samples for each subject (26 images per subject versus 64 images per subject). Thirdly, we investigated two kinds of corruption, white noise (additive noise) and random pixel corruption (non-additive noise) which are two commonly assumed in face recognition problem [1, 2]. For the white noise case (the top row of Figure 7), we add random noise from normal distribution to each testing image \mathbf{x} , that is, $\tilde{\mathbf{x}} = \mathbf{x} + \alpha \mathbf{n}$, and restrict $\tilde{\mathbf{x}} \in [0, 255]$, where

α is the corruption ratio from 10% to 100% with an interval of 10%, and \mathbf{n} is the noise following a standard normal distribution. For the random pixel corruption case (the bottom row in Figure 7), we replace the value of a percentage of pixels randomly chosen from each test image with the values following a uniform distribution over $[0, p_{max}]$, where p_{max} is the largest pixel value of current image.

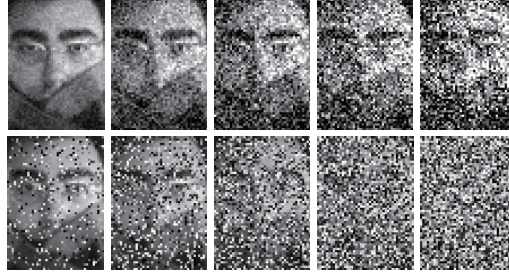


Figure 7: Testing images from AR database with corruption. Top row: 10%, 30%, 50%, 70%, 90% white noises are added into test image; Bottom row, 20%, 40%, 60%, 80%, 100% of pixels are randomly corrupted.

Table 4: The robustness to white gaussian noise using Eigenface (300D) on the AR database (coding over \mathbf{D}).

Corruption ratio	10%	20%	30%	40%	50%	60%	70%	80%	90%	100%
SVM [38]	91.77%	91.46%	91.38%	91.15%	90.23%	89.85%	88.62%	86.08%	82.69%	80.08%
SRC [1]	92.62%	91.54%	91.23%	89.23%	86.54%	82.54%	78.31%	72.08%	62.62%	56.46%
ℓ^2 -FR [2]	93.39%	92.92%	92.39%	91.23%	88.85%	85.23%	81.85%	75.54%	67.62%	62.23%
CRC-RLS [3]	94.77%	94.46%	94.39%	94.15%	92.85%	91.77%	90.92%	89.23%	87.31%	84.92%
LCCR + Cityblock	97.00%	96.08%	96.00%	95.62%	94.54%	94.15%	92.31%	90.85%	89.08%	87.39%
LCCR + Seucclidean	96.31%	95.77%	95.77%	95.54%	94.46%	94.39%	92.39%	90.85%	88.54%	86.69%
LCCR + Euclidean	95.77%	95.46%	95.23%	95.15%	94.23%	94.08%	92.31%	90.77%	88.31%	86.54%
LCCR + Cosine	95.62%	95.15%	95.15%	95.08%	93.92%	93.85%	92.15%	90.31%	88.69%	86.92%
LCCR + Spearman	96.15%	95.46%	95.39%	95.15%	94.69%	94.23%	93.08%	92.15%	89.77%	89.00%

Table 5: The robustness to white gaussian noises using Eigenface (300D) on the AR database (coding over $[\mathbf{D} \mathbf{I}]$).

Corruption ratio	10%	20%	30%	40%	50%	60%	70%	80%	90%	100%
SRC [1]	92.62%	91.77%	92.23%	91.08%	90.46%	89.39%	87.92%	84.15%	84.08%	78.92%
ℓ^2 -FR [2]	92.62%	92.23%	92.15%	91.92%	91.00%	90.62%	88.85%	87.31%	86.31%	82.15%
CRC-RLS [3]	92.62%	92.23%	92.15%	91.92%	91.00%	90.69%	88.85%	87.31%	86.31%	82.15%
LCCR + Cityblock	93.08%	92.92%	92.85%	92.39%	91.69%	91.15%	89.62%	88.08%	86.62%	84.23%
LCCR + Seucclidean	92.92%	92.85%	92.62%	92.39%	91.69%	91.23%	89.62%	88.15%	86.46%	83.62%
LCCR + Euclidean	92.85%	92.77%	92.54%	92.39%	91.69%	91.39%	89.92%	88.31%	86.62%	83.46%
LCCR + Cosine	92.77%	92.69%	92.69%	92.62%	91.92%	91.69%	89.92%	88.39%	87.00%	83.85%
LCCR + Spearman	93.00%	92.85%	92.85%	92.85%	92.15%	91.62%	90.15%	89.54%	87.54%	86.39%

Table 6: The robustness to white gaussian noises using the AR database (2580D) (coding over \mathbf{D}).

Corruption ratio	10%	20%	30%	40%	50%	60%	70%	80%	90%	100%
SVM [38]	91.92%	91.92%	91.69%	91.31%	90.00%	89.85%	88.62%	85.62%	82.92%	79.85%
ℓ^2 -FR [2]	78.69%	55.23%	33.77%	17.00%	4.62%	3.38%	4.62%	3.38%	2.69%	2.31%
CRC-RLS [3]	94.92%	94.85%	94.77%	93.92%	93.23%	92.23%	90.85%	89.31%	88.39%	85.39%
LCCR + Cityblock	97.54%	96.54%	96.08%	95.85%	95.08%	94.92%	93.15%	91.54%	90.54%	86.77%
LCCR + Seucclidean	96.92%	96.23%	96.08%	95.92%	95.39%	94.62%	92.92%	91.15%	89.00%	87.00%
LCCR + Euclidean	96.08%	95.62%	95.46%	95.39%	94.85%	94.23%	92.23%	91.31%	88.92%	87.08%
LCCR + Cosine	96.08%	95.62%	95.46%	95.31%	94.39%	94.31%	92.54%	90.62%	89.46%	87.23%
LCCR + Spearman	96.54%	95.77%	95.62%	95.23%	94.69%	94.54%	93.31%	92.23%	90.39%	89.39%

To improve the anti-noise ability of SRC [1], Wright et al. generate a new dictionary $[\mathbf{D} \mathbf{I}]$ by concatenating an identity matrix \mathbf{I} with the original dictionary \mathbf{D} , where the dimensionality of \mathbf{I} equals to that of data. The use

Table 7: The robustness to white gaussian noises using the AR database (2580D) (coding over **[D I]**).

Corruption ratio	10%	20%	30%	40%	50%	60%	70%	80%	90%	100%
ℓ^2 -FR [2]	93.00%	93.00%	92.46%	92.77%	91.69%	90.92%	90.15%	88.15%	87.15%	83.08%
CRC-RLS [3]	93.00%	93.00%	92.46%	92.77%	91.69%	90.92%	89.23%	88.15%	87.15%	83.08%
LCCR + Cityblock	93.39%	93.31%	93.31%	93.00%	92.15%	91.85%	90.15%	88.77%	87.39%	85.31%
LCCR + Seuclidean	93.39%	93.00%	93.00%	92.40%	92.15%	91.69%	90.15%	88.77%	87.31%	84.39%
LCCR + Euclidean	93.31%	93.08%	93.23%	92.77%	91.92%	91.77%	90.31%	88.85%	87.62%	84.46%
LCCR + Cosine	93.15%	93.08%	93.08%	93.00%	92.23%	92.08%	90.39%	89.39%	87.77%	84.46%
LCCR + Spearman	93.54%	93.39%	93.39%	93.15%	92.62%	92.15%	90.54%	90.23%	88.31%	87.08%

Table 8: The robustness to random pixel corruption using Eigenface (300D) on the AR database (coding over **D**).

Corruption ratio	10%	20%	30%	40%	50%	60%	70%	80%	90%	100%
SVM [38]	91.54%	88.00%	81.92%	66.54%	45.46%	23.00%	8.23%	3.69%	2.00%	1.15%
SRC [1]	89.62%	84.31%	72.31%	55.15%	38.85%	20.31%	8.23%	4.62%	2.00%	1.00%
ℓ^2 -FR [2]	91.77%	86.62%	77.00%	62.08%	45.77%	28.46%	13.62%	4.77%	2.54%	1.54%
CRC-RLS [3]	84.08%	91.62%	88.69%	80.23%	65.46%	44.77%	20.77%	6.69%	2.92%	1.62%
LCCR + Cityblock	96.54%	95.23%	92.31%	87.77%	79.69%	62.31%	37.08%	15.39%	5.23%	1.62%
LCCR + Seuclidean	95.69%	93.39%	90.08%	81.92%	65.85%	44.85%	20.77%	1.46%	3.00%	1.69%
LCCR + Euclidean	95.39%	92.85%	90.39%	82.85%	67.23%	45.08%	20.92%	6.69%	3.23%	1.62%
LCCR + Cosine	94.85%	92.46%	89.46%	81.39%	65.62%	45.08%	20.85%	6.77%	3.69%	2.08%
LCCR + Spearman	95.54%	94.08%	92.54%	88.62%	83.00%	74.15%	59.31%	38.00%	13.69%	1.92%

Table 9: The robustness to random pixel corruption using Eigenface (300D) on the AR database (coding over **[D I]**).

Corruption ratio	10%	20%	30%	40%	50%	60%	70%	80%	90%	100%
SRC [1]	91.62%	88.85%	83.38%	73.92%	56.31%	33.08%	14.92%	4.92%	2.08%	1.31%
ℓ^2 -FR [2]	91.15%	89.46%	84.46%	71.31%	49.92%	25.69%	8.31%	2.92%	1.85%	1.15%
CRC-RLS [3]	91.15%	89.46%	84.46%	71.31%	49.92%	25.69%	8.31%	2.92%	1.85%	1.15%
LCCR + Cityblock	92.62%	90.92%	87.54%	81.15%	69.46%	53.08%	34.00%	14.62%	4.92%	1.38%
LCCR + Seuclidean	91.85%	89.77%	85.23%	72.39%	50.00%	25.92%	8.31%	3.31%	2.46%	1.31%
LCCR + Euclidean	91.92%	89.85%	85.15%	73.23%	51.23%	27.62%	10.23%	4.00%	2.54%	1.31%
LCCR + Cosine	92.15%	90.00%	84.92%	71.46%	49.92%	25.69%	8.38%	5.31%	2.62%	1.23%
LCCR + Spearman	92.69%	90.85%	87.85%	83.08%	75.92%	66.69%	56.54%	37.85%	1.38%	1.77%

Table 10: The robustness to random pixel corruption using the AR database (2580D) (coding over **D**).

Corruption ratio	10%	20%	30%	40%	50%	60%	70%	80%	90%	100%
SVM [38]	91.69%	88.38%	81.46%	65.62%	44.77%	22.23%	7.69%	3.69%	1.92%	1.23%
ℓ^2 -FR [2]	21.77%	8.31%	3.77%	3.23%	2.39%	1.92%	0.92%	1.23%	1.15%	1.00%
CRC-RLS [3]	94.15%	92.00%	89.08%	82.00%	67.08%	47.08%	22.69%	7.00%	2.62%	1.23%
LCCR + Cityblock	96.85%	95.62%	93.23%	88.62%	78.77%	57.54%	29.77%	8.08%	4.54%	1.62%
LCCR + Seuclidean	96.00%	94.23%	90.77%	82.85%	67.31%	47.08%	22.69%	7.15%	3.00%	1.54%
LCCR + Euclidean	95.62%	93.62%	91.15%	83.77%	68.31%	47.39%	22.92%	7.15%	3.00%	1.54%
LCCR + Cosine	95.31%	93.31%	90.77%	82.62%	67.15%	47.15%	23.23%	7.23%	3.62%	1.77%
LCCR + Spearman	95.85%	94.77%	92.92%	89.23%	83.31%	74.77%	60.69%	38.00%	13.85%	1.85%

Table 11: The robustness to random pixel corruption using the AR database (2580D) (coding over **[D I]**).

Corruption ratio	10%	20%	30%	40%	50%	60%	70%	80%	90%	100%
ℓ^2 -FR [2]	92.15%	89.85%	84.92%	73.15%	51.15%	26.15%	8.54%	2.92%	1.77%	1.15%
CRC-RLS [3]	92.15%	89.85%	84.92%	73.15%	51.15%	26.15%	8.54%	3.00%	1.77%	1.15%
LCCR + Cityblock	93.08%	91.39%	88.23%	81.92%	70.15%	53.54%	34.08%	14.62%	5.08%	1.38%
LCCR + Seuclidean	92.69%	90.39%	85.85%	73.85%	51.39%	26.15%	8.62%	3.31%	2.46%	1.31%
LCCR + Euclidean	92.62%	90.39%	86.00%	74.46%	52.46%	28.54%	10.69%	4.08%	2.54%	1.38%
LCCR + Cosine	92.69%	90.54%	85.62%	73.15%	51.59%	26.15%	8.62%	6.08%	2.77%	1.31%
LCCR + Spearman	93.31%	91.54%	88.54%	84.31%	77.00%	67.00%	56.54%	37.85%	13.62%	1.62%

of **I** has been verified to be effective in improving the robustness of ℓ^1 -norm based models [13, 42], while it will increase the computational costs. Therefore, this is a tradeoff between robustness and computational efficiency for

these algorithms. Will the strategy still work for ℓ^2 -minimization based models? In this sub-section, we fill this gap by comparing the results by coding over these two dictionary.

Table 4 through Table 11 are the recognition rates of the tested methods across feature space (Eigenface with 300D) and full dimensional space (2580D). The results of SVM with the strategy of expanding dictionary are not reported as SVM is directly conducted on the input without encoding. Based on the results, we have the following conclusions:

Firstly, the proposed LCCRs are much superior to SVM, SRC, ℓ^2 -FR and CRC-RLS with considerable margins in various tests. For example, in the worst case (the white noise corruption ratio is 100%, Table 4-7), the best result of LCCR, which is achieved with Spearman distance, is about 89.39% (Table 6), compared to 80.08% for SVM (Table 4), 78.92% for SRC (Table 5), 83.05% for ℓ^2 -FR (Table 5), and 85.39% for CRC-RLS (Table 6). In the case of random pixel corruption (Table 8-11), one can see when the corruption ratio reaches 70%, all methods fail to perform recognition except LCCR whose best result is about 60.69% (Table 10), compared to 8.23% for SVM (Table 8), 14.92% for SRC (Table 9), 13.62% for ℓ^2 -FR (Table 8), and 22.69% for CRC-RLS (Table 10).

Secondly, all investigated algorithms perform worse with increased corruption ratio, and achieve better results in white noise corruption (additive noise) than random pixel corruption (non-additive noise). Moreover, all models perform slightly better (less than 1%) over full-dimensional space excepted ℓ^2 -FR.

Thirdly, the results show that coding over $[\mathbf{D} \ \mathbf{I}]$ is helpful in improving the robustness of SRC and ℓ^2 -FR, but it has negative impact on the recognition accuracy of CRC-RLS and LCCR. For example, when white noise ratio rises to 100% for the Eigenface (Table 4 and 5), expanding \mathbf{D} leads to the variation of the recognition rate from 56.46% to 78.92% for SRC, from 62.23% to 82.15% for ℓ^2 -FR, from 84.92% to 82.12% for CRC-RLS, and from 89.00% to 86.39% for LCCR with Spearman distance. This result has not been reported in previous works.

5. Conclusions and Discussions

It is interesting and important to improve the discrimination and robustness of data representation. The traditional coding algorithm gets the representation by coding each datum as a linear combination of a set of training set, which depicts the global structure and property of data. However, it will be failed when the data are corrupted. Locality preservation has shown the effectiveness in revealing the structure of data, which could keep the geometric structure of manifold. In this paper, we proposed a novel objective function to get an effective and robust representation by incorporating the locality into the coding scheme, and the function possesses analytic solution. Moreover, two recent proposed models, ℓ^2 -FR and CRC-RLS, could be regarded as two special versions of our model without locality constraint. The experimental studies showed that the introduction of locality makes LCCR more accurate and robust to various occlusions and corruptions. We analyze the classification results of LCCR with five basic distance metrics (for locality). The results imply that if better K -NN searching methods or more sophisticated distance metrics are adopted, such as, the supervised distance metric learning [43], LCCR will achieve higher recognition result and better robustness. Moreover, the performance comparisons over two different dictionaries show that it is unnecessary to expand the dictionary \mathbf{D} with \mathbf{I} for ℓ^2 -norm based coding algorithms.

Each approach has its own advantages and disadvantages. Parameter determination maybe is the biggest problem of LCCR which requires the specification of three parameters, locality parameter K and two constraint parameters λ and γ . In the future works, we will focus on some of these issues. For example, it is possible that the value of K can refer to the intrinsic dimensionality of subspace. Moreover, dictionary learning plays an important role in information representation. Hence, it is valuable to explore how to exploit low-dimensional geometric models to build an effective dictionary.

References

- [1] J. Wright, A. Y. Yang, A. Ganesh, S. S. Sastry, Y. Ma, Robust face recognition via sparse representation, *IEEE Transactions on Pattern Analysis and Machine Intelligence* 31 (2) (2009) 210–227.
- [2] S. Qinfeng, A. Eriksson, A. van den Hengel, S. Chunhua, Is face recognition really a compressive sensing problem?, in: *Proc. of IEEE International Conference on Computer Vision and Pattern Recognition (CVPR)*, 2011, pp. 553–560.
- [3] L. Zhang, M. Yang, X. Feng, Sparse representation or collaborative representation: Which helps face recognition?, in: *Proc. of IEEE International Conference on Computer Vision (ICCV)*, 2011.

- [4] B. A. Olshausen, D. J. Field, Emergence of simple-cell receptive field properties by learning a sparse code for natural images, *Nature* 381 (6583) (1996) 607–609.
- [5] M. Riesenhuber, T. Poggio, Hierarchical models of object recognition in cortex, *Nature Neuroscience* 2 (11) (1999) 1019–1025.
- [6] D. L. Donoho, M. Elad, Optimally sparse representation in general (nonorthogonal) dictionaries via ℓ^1 minimization, *Proceedings of the National Academy of Sciences* 100 (5) (2003) 2197–2202.
- [7] E. J. Candes, T. Tao, Decoding by linear programming, *IEEE Transactions on Information Theory* 51 (12) (2005) 4203–4215.
- [8] D. L. Donoho, For most large underdetermined systems of linear equations the minimal ℓ^1 -norm solution is also the sparsest solution, *Communications on Pure and Applied Mathematics* 59 (6) (2006) 797–829.
- [9] C. S. S., D. L. Donoho, M. A. Saunders, Atomic decomposition by basis pursuit, *Siam Review* 43 (1) (2001) 129–159.
- [10] B. Efron, T. Hastie, I. Johnstone, R. Tibshirani, Least angle regression, *Annals of Statistics* 32 (2) (2004) 407–451.
- [11] A. Yang, S. Sastry, A. Ganesh, Y. Ma, Fast ℓ^1 -minimization algorithms and an application in robust face recognition: A review, in: *Proc. of IEEE International Conference on Image Processing (ICIP)*, IEEE, 2010, pp. 1849–1852.
- [12] E. Elhamifar, R. Vidal, Sparse manifold clustering and embedding, in: *Proc. Advances in Neural Information Processing Systems*, 2011.
- [13] L. S. Qiao, S. C. Chen, X. Y. Tan, Sparsity preserving projections with applications to face recognition, *Pattern Recognition* 43 (1) (2010) 331–341.
- [14] J. Gui, Z. Sun, W. Jia, R. Hu, Y. Lei, S. Ji, Discriminant sparse neighborhood preserving embedding for face recognition, *Pattern Recognition* 45 (8) (2012) 2884 – 2893. doi:10.1016/j.patcog.2012.02.005.
- [15] B. Cheng, J. Yang, S. Yan, Y. Fu, T. Huang, Learning with ℓ^1 -graph for image analysis, *IEEE Transactions on Image Processing* 19 (4) (2010) 858–866.
- [16] E. Elhamifar, R. Vidal, Sparse subspace clustering: Algorithm, theory, and applications, *Arxiv preprint arXiv:1203.1005*.
- [17] Y. Kai, L. Yuanqing, J. Lafferty, Learning image representations from the pixel level via hierarchical sparse coding, in: *Proc. of IEEE International Conference on Computer Vision and Pattern Recognition (CVPR)*, 2011, pp. 1713–1720.
- [18] P. Hoyer, Non-negative matrix factorization with sparseness constraints, *The Journal of Machine Learning Research* 5 (2004) 1457–1469.
- [19] J. Yang, L. Zhang, Y. Xu, J. Yang, Beyond sparsity: The role of l1-optimizer in pattern classification, *Pattern Recognition* 45 (3) (2012) 1104–1118.
- [20] R. Rigamonti, M. A. Brown, V. Lepetit, Are sparse representations really relevant for image classification?, in: *Proc. of IEEE International Conference on Computer Vision and Pattern Recognition (CVPR)*, 2011, pp. 1545–1552.
- [21] S. T. Roweis, L. K. Saul, Nonlinear dimensionality reduction by locally linear embedding, *Science* 290 (5500) (2000) 2323–2326. doi:10.1126/science.290.5500.2323.
- [22] M. Belkin, P. Niyogi, Laplacian eigenmaps for dimensionality reduction and data representation, *Neural Computation* 15 (6) (2003) 1373–1396.
- [23] X. He, D. Cai, S. Yan, H. Zhang, Neighborhood preserving embedding, in: *Proc. of IEEE International Conference on Computer Vision (ICCV)*, Vol. 2, IEEE, 2005, pp. 1208–1213.
- [24] S. C. Yan, D. Xu, B. Y. Zhang, H. J. Zhang, Q. Yang, S. Lin, Graph embedding and extensions: A general framework for dimensionality reduction, *IEEE Transactions on Pattern Analysis and Machine Intelligence* 29 (1) (2007) 40–51.
- [25] J. Yang, D. Zhang, J. Y. Yang, B. Niu, Globally maximizing, locally minimizing: Unsupervised discriminant projection with applications to face and palm biometrics, *IEEE Transactions on Pattern Analysis and Machine Intelligence* 29 (4) (2007) 650–664.
- [26] R. G. Baraniuk, M. B. Wakin, Random projections of smooth manifolds, *Foundations of Computational Mathematics* 9 (1) (2006) 941–944.
- [27] A. Majumdar, R. K. Ward, Robust classifiers for data reduced via random projections, *IEEE Transactions on Systems, Man, and Cybernetics, Part B: Cybernetics* 40 (5) (2010) 1359–1371. doi:10.1109/TSMCB.2009.2038493.
- [28] P. Xi, L. Zhang, Z. Yi., Constructing l2-graph for subspace learning and segmentation, *ArXiv e-prints arXiv:1209.0841*.
- [29] W. Jinjun, Y. Jianchao, Y. Kai, L. Fengjun, T. Huang, G. Yihong, Locality-constrained linear coding for image classification, in: *Proc. of IEEE International Conference on Computer Vision and Pattern Recognition (CVPR)*, 2010, pp. 3360–3367.
- [30] Y. Chao, Y. Yeh, Y. Chen, Y. Lee, Y. Wang, Locality-constrained group sparse representation for robust face recognition, in: *Proc. of IEEE International Conference on Image Processing (ICIP)*, IEEE, 2011, pp. 761–764.
- [31] M. Yang, L. Zhang, D. Zhang, S. Wang, Relaxed collaborative representation for pattern classification, in: *Proc. of IEEE Conference on Computer Vision and Pattern Recognition (CVPR)*, 2012, pp. 2224–2231.
- [32] L. Yang, Distance metric learning: A comprehensive survey, Tech. rep., Carnegie Mellon University (2006).
- [33] A. Martinez, R. Benavente, The AR face database, Tech. rep., The Ohio State University (1998).
- [34] F. Samaria, A. Harter, Parameterisation of a stochastic model for human face identification, in: *the IEEE Workshop on Applications of Computer Vision (WACV)*, 1994, pp. 138–142. doi:10.1109/ACV.1994.341300.
- [35] A. Georgiades, P. Belhumeur, D. Kriegman, From few to many: illumination cone models for face recognition under variable lighting and pose, *IEEE Transactions on Pattern Analysis and Machine Intelligence* 23 (6) (2001) 643–660. doi:10.1109/34.927464.
- [36] P. Phillips, H. Moon, S. Rizvi, P. Rauss, The feret evaluation methodology for face-recognition algorithms, *IEEE Transactions on Pattern Analysis and Machine Intelligence* 22 (10) (2000) 1090–1104.
- [37] P. Phillips, P. Flynn, T. Scruggs, K. Bowyer, J. Chang, K. Hoffman, J. Marques, J. Min, W. Worek, Overview of the face recognition grand challenge, in: *Proc. of IEEE Conference on Computer Vision and Pattern Recognition (CVPR)*, Vol. 1, IEEE, 2005, pp. 947–954.
- [38] R.-E. Fan, K.-W. Chang, C.-J. Hsieh, X.-R. Wang, C.-J. Lin, Liblinear: A library for large linear classification, *Journal of Machine Learning Research* 9 (2008) 1871–1874.
- [39] M. Grant, S. Boyd, Graph implementations for nonsmooth convex programs, in: V. Blondel, S. Boyd, H. Kimura (Eds.), *Recent Advances in Learning and Control, Lecture Notes in Control and Information Sciences*, Springer-Verlag Limited, 2008, pp. 95–110.
- [40] M. Savvides, R. Abiantun, J. Heo, S. Park, C. Xie, B. Vijayakumar, Partial holistic face recognition on frgc-ii data using support vector machine, in: *Computer Vision and Pattern Recognition Workshop (CVPRW)*, 2006, pp. 48–53. doi:10.1109/CVPRW.2006.153.
- [41] P. Sinha, B. Balas, Y. Ostrovsky, R. Russell, Face recognition by humans: Nineteen results all computer vision researchers should know about, *Proceedings of the IEEE* 94 (11) (2006) 1948–1962.

- [42] J. Wright, Y. Ma, J. Mairal, G. Sapiro, T. Huang, S. Yan, Sparse representation for computer vision and pattern recognition, *Proceedings of the IEEE* 98 (6) (2010) 1031–1044. doi:10.1109/JPROC.2010.2044470.
- [43] S. Chopra, R. Hadsell, Y. LeCun, Learning a similarity metric discriminatively, with application to face verification, in: *Proc. of IEEE International Conference on Computer Vision and Pattern Recognition (CVPR)*, Vol. 1, 2005, pp. 539–546.